Redefine Sustainable Fisheries Targets Under the Impact of the Southern Yellow Sea Green Tide: Mitigating the Recurring Surge in Natural Mortality

Ming Sun[1,2], Yunzhou Li[1,2], Yiping Ren[1,3,4]* and Yong Chen[2]

[1] College of Fisheries, Ocean University of China, Qingdao, China, [2] School of Marine and Atmospheric Sciences, Stony Brook University, Stony Brook, NY, United States, [3] Field Observation and Research Station of Haizhou Bay Fishery Ecosystem, Ministry of Education of the People's Republic of China, Qingdao, China, [4] Laboratory for Marine Fisheries Science and Food Production Processes, Pilot National Laboratory for Marine Science and Technology (Qingdao), Qingdao, China

The massive green tide blooms caused by macroalgae *Ulva* in the Southern Yellow Sea, China, threaten the local fish populations. However, green tides are not factored into the determination of sustainable fisheries targets, which hinders the achievement of the maximum sustainable yield (MSY). Using a local fishery as a case study we highlighted the need to redefine the MSY-based targets in the face of green tides. We modeled the green tide blooms as natural mortality events and evaluated their effects on fisheries with the "green-tide-free" sustainable fishing intensity F_{MSY}. We then recalculated these targets by accounting for the surges in natural mortality. We found that green tides caused at least 10% losses in biomass and catch when unaccounted for. Additionally, F_{MSY} must be reduced by 4–8% to achieve MSY in the face of the green tide, which was approximately 20% lower than the "green-tide-free" value, indicating the damages of green tides could be partially mitigated.

Keywords: green tide, harmful algal bloom, natural mortality, sustainable fisheries, Yellow Sea

INTRODUCTION

Harmful Algal Blooms (HABs) have been increasingly occurring in recent years worldwide, threatening the well-being of fish stocks and fisheries (Burkholder, 1998; Zhang J. et al., 2019; Liu et al., 2021a,b; Zhuang et al., 2021). From the perspective of fisheries ecology, HABs are considered as an event that can cause dramatic surge in natural morality of fish, which is not only hard to quantify in retrospect but also hard to predict in advance (Ward and Tunnell, 2017). As a socio-economic and ecological interfaced sector, capture fisheries can be susceptible to HABs even when well managed. For example, fish kills due to red tides are among the most critical ecological issues in the Gulf of Mexico (Cruz-Rivera et al., 2015; Ward and Tunnell, 2017; Harford et al., 2018). The severe red-tide event in 2005 caused a quadrupled natural mortality for the Gulf of Mexico red grouper, which translated into the fish biomass loss of 11,000 mt (Southeast Data, Assessment, and Review [SEDAR], 2015). The summer-long HAB in the Lake Erie from 2011 to 2014 resulted in more than five million dollars loss for the local recreational fishery (Wolf et al., 2017). Commercial

shellfish fisheries in the Gulf of Maine and North American West Coast were also strongly impacted by local HABs events and suffered economic losses (Jin and Hoagland, 2008; McCabe et al., 2016). The red tides in the Seto Inland Sea, Japan, has been causing huge fishery damages in natural bivalves for more than four decades (Imai et al., 2006; Imai and Yamaguchi, 2012).

Factoring the influence of HABs into fisheries management is crucial to the achievement of sustainable fisheries (Burkholder, 1998). The definitions and operational targets of sustainable fisheries may vary by case, but the fundamental idea is to fish at an optimal level to maximize the yield without compromising the stock productivity to preserve the long-term yield, defined as maximum sustainable yield (MSY) (Beverton and Holt, 1957). The MSY can also be defined with the fishing mortality (F) imposed on the stock (i.e., F_{MSY}) and the equilibrium stock biomass (B) supporting MSY (B_{MSY}). Natural mortality is a key vital rate in estimating these quantities. However, this is challenging in the face of HABs. Natural mortality is difficult to estimate; most practical stock assessment often assumes it as invariants (Brodziak et al., 2011; Then et al., 2015). Additionally, distinguishing HABs-related mortality from the total natural mortality is even more difficult, since the direct link between natural mortality and HABs is vague. Previous approach to incorporate HAB into fisheries population dynamics is to treat it as a natural mortality event (Harford et al., 2018). The increases in natural mortality were assumed to be related to the intensity of HABs, linked by a standardized index quantifying intensity of blooms (Walter et al., 2013; Southeast Data, Assessment, and Review [SEDAR], 2015). Nevertheless, this method was only used to advise modifications of pre-existing catch limits (Harford et al., 2018), not to address more general concerns in defining targets for sustainable fisheries.

The green tide in the South Yellow Sea, China, caused by the expansion of *Ulva prolifera* is the largest HABs ever reported for macroalgae (Liu et al., 2013). Since the first appearance in 2007, green tides have occurred for more than 15 consecutive years offshore Jiangsu and Shandong provinces (Liu et al., 2010; Zhang Y. et al., 2019). The recurrence of the green tide has a rather consistent temporal pattern: the bloom-forming *U. prolifera* starts to dominate the small-scale local algal community in the southern part of the Yellow Sea in late April to early May, and then moves northward under the influence of wind and currents, followed by massive blooms in the whole coastal area to the south of the Shandong peninsular in June and July (Sun et al., 2008; Zhou et al., 2015; Zhang Y. et al., 2019). Satellite and field observations indicate that the green tide biomass originates from the *Neopyropia* maricultural facilities (particularly rafts), which serve as nurseries for *U. prolifera* (Liu et al., 2010, 2021c, 2022; Zhang Y. et al., 2019). When the synergistic effects of environmental factors such as temperature, light intensity, and wind are suitable, *U. prolifera* would proliferate and rapidly develop into large-scale HABs (Cui et al., 2015; Gao et al., 2017). The local eutrophication level is also considered a major contributor to the periodically recurring blooms, which is reported to exacerbate in recent years due to the growing inputs from land and aquaculture wastes (Xing et al., 2015;

Zhang et al., 2015). The socio-economic damages caused by the Yellow Sea green tide are substantial. The unprecedented bloom in 2008 inflicted a considerable direct economic loss of 2.8 billion RMB (~440 million USD), including the 2 billion RMB governmental expenditures to handle the floating algal mat and the 800 million RMB direct economic losses of the local aquaculture industry (Ye et al., 2011). Green tides also bring great environmental harm to the Yellow Sea. Documented changes in environmental indicators include increased seawater pH, decreased oxygen concentration rate, and increased bacterial abundance (Zhang Y. et al., 2019). The consequent hypoxia and acidification may take tolls on the entire marine ecosystem (Backer, 2009; Ye et al., 2011; Lewitus et al., 2012; Glibert et al., 2014).
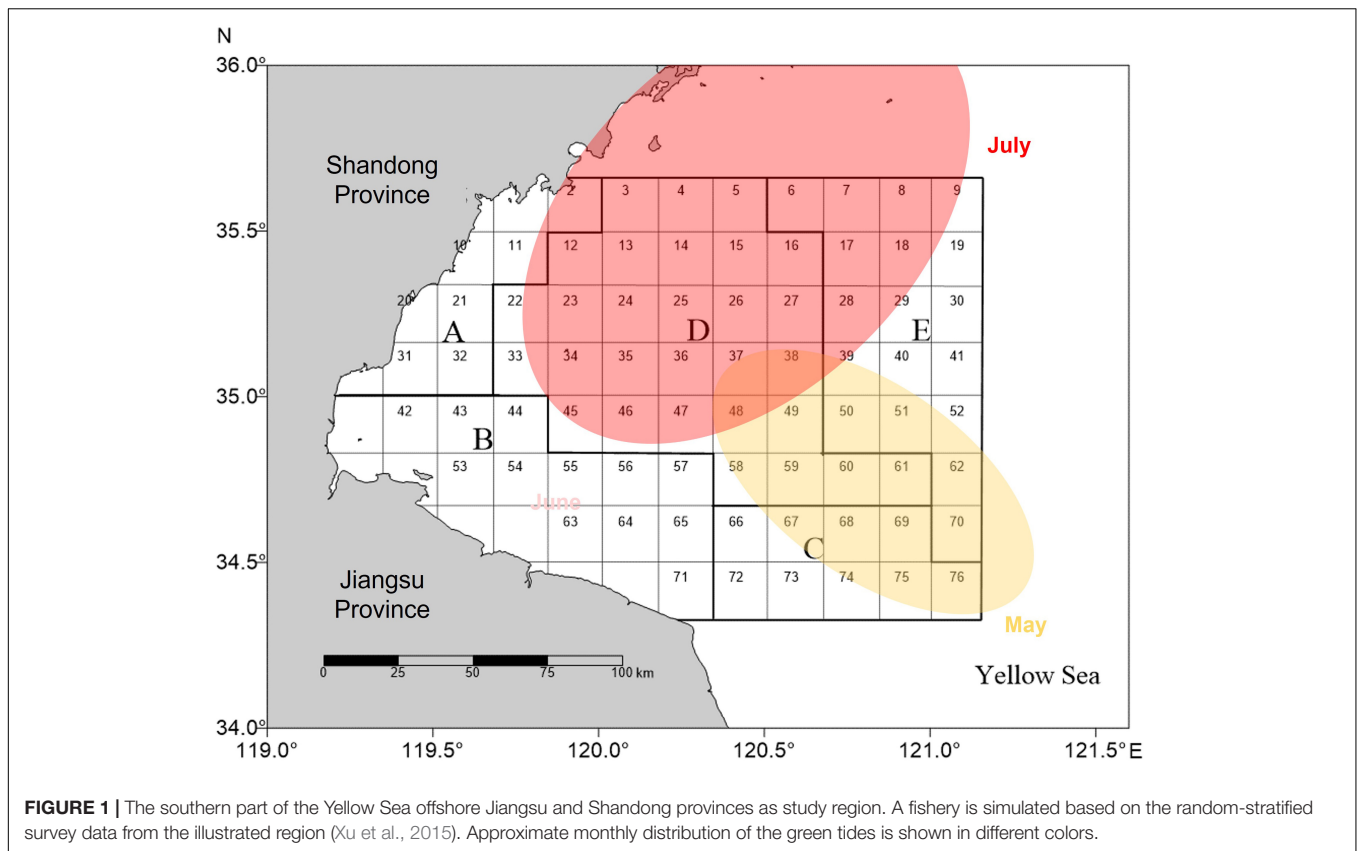
Unfortunately, there are no assessments on the green tide's effects to the Southern Yellow Sea fisheries. Given that the Yellow Sea contributes more than 25 million tons of marine fisheries catch (MARA, 2018), the increased natural mortality due to green tides could have already impacted the status of fish population as well as the yields. We do not have adequate information on the Yellow Sea fisheries and the green tides to include green tides in stock assessment, not to mention to assess their impact to fisheries management. Recent studies based on data-limited methods have defined model-based sustainable targets (such as F_{MSY} and B_{MSY}) for some fisheries in the Southern Yellow Sea and showed that the biomass of major commercial fisheries is below the B_{MSY} level (Sun et al., 2018a,b; Wang et al., 2020). However, it is still largely unknown to what extent green tides contribute to the loss as they were never considered in the process of developing fisheries management regulations and stock assessment, rendering the previously defined F_{MSY} and MSY less reliable.

The present study uses a fishery in the Southern Yellow Sea as a case study, aiming to evaluate the biomass and catch losses of fisheries under predefined F_{MSY} and MSY in the face of green tides, and redefine their values by accounting for green tide blooms. The green tide blooms are modeled as an event that cause periodically recurring surges in natural mortality for the fish population. The outbreak period of green tides is modeled based on its relatively consistent temporal patterns (Sun et al., 2008; Zhou et al., 2015; Zhang Y. et al., 2019). The magnitude of surge in natural mortality rates is related to the intensity of green tide blooms based on the historical data. Influences of green tides on the fishery are projected under different bloom intensities. Through the simulation, we expect to highlight the damages in the Southern Yellow Sea fishery due to green tides that were not well studied and understood and provide guidance for improved estimation of sustainable fisheries yields.

MATERIALS AND METHODS

Study Region and Data

We focused our study on the southern part of the Yellow Sea offshore Jiangsu and Shandong provinces (**Figure 1**). This region was selected because commercial fishing and green tide

FIGURE 1 | The southern part of the Yellow Sea offshore Jiangsu and Shandong provinces as study region. A fishery is simulated based on the random-stratified survey data from the illustrated region (Xu et al., 2015). Approximate monthly distribution of the green tides is shown in different colors.

outbreaks were overlapped according to previous observation and monitoring (Xu et al., 2015; Zhang Y. et al., 2019). We used the historical green tide records since 2007 from a series of publications to derive the intensity of bloom by year (Liu et al., 2013; Zhou et al., 2015; Zhang Y. et al., 2019). The intensity of the blooms was primarily measured with the size of algal distribution area (**Figure 2A**). The data for the fishery in the region were provided by a fisheries-independent survey (Xu et al., 2015). The survey followed a random-stratified station design and has provided sufficient data to support the development of a fisheries projection simulator which was used in this study as the simulation platform (Sun et al., 2021a). Other than this, fisheries in the Southern Yellow Sea were subject to limited data, resulting in the lack of formal stock assessment and harvest control rules (Sun et al., 2018a). We simulated a fishery in the region based on the small yellow croaker fishery (*Larimichthys polyactis*). We linked the green tide blooms to the population dynamics of the fishery and performed simulations under different bloom intensities to showcase the dynamics of fisheries under the impact of green tides.

Linking Natural Mortality With Green Tide Bloom

Green tides can affect fish populations in many ways. In this study, the green tide bloom was modeled as a periodical recurring event, based on the data we had, that caused surge in natural
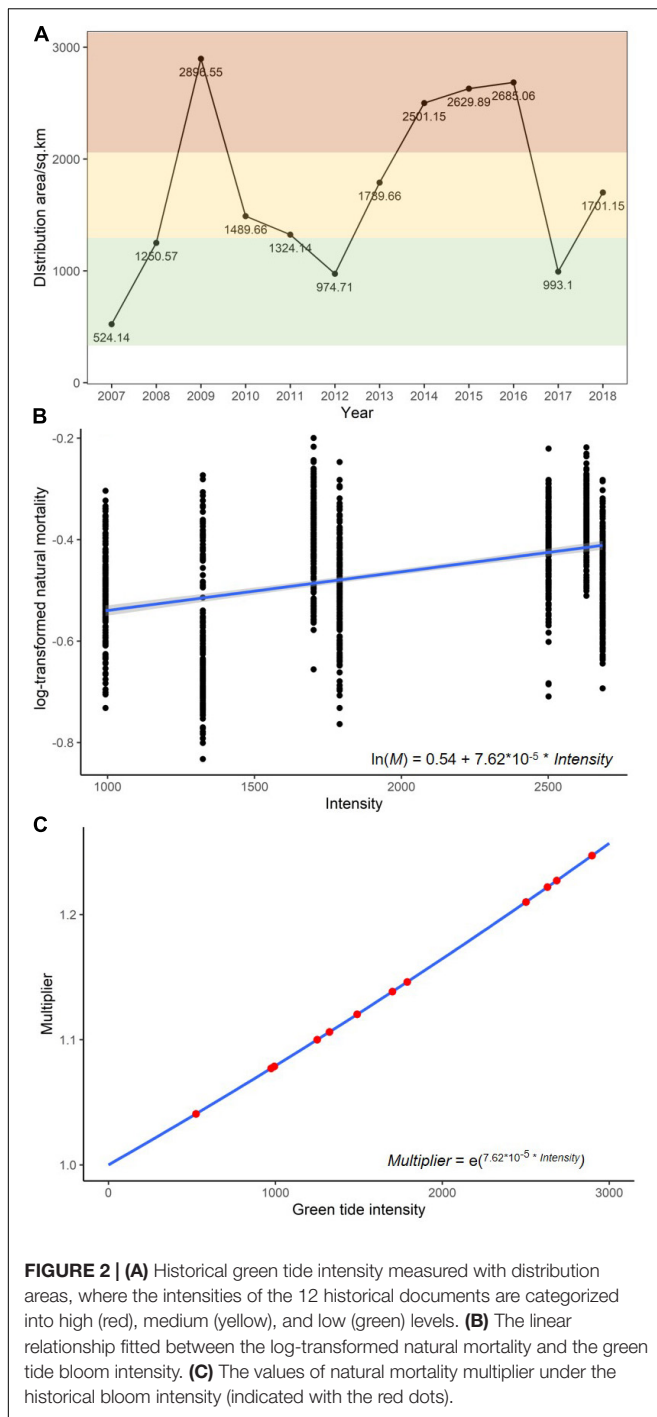
mortality rates (M) of the fish stock. This approach has been adopted to advise fisheries management in the Gulf of Mexico to counter the substantial fish kills due to the local harmful red tide blooms (Southeast Data, Assessment, and Review [SEDAR], 2015; Harford et al., 2018).

In the realm of stock assessment, M was notoriously difficult to determine. Prevailingly, empirical methods developed from metadata were used as the most reliant approach to provide M estimates, which would be subject to large prediction errors at the case-specific level (Then et al., 2015). To cope with this issue, we designed a workflow to repetitively generate a range of M estimates for each year with available data. The workflow started by estimating von Bertalanffy growth parameters (asymptotic length L and growth rate K) with the genetic algorithm-based electronic length frequency analysis (Taylor and Mildenberger, 2017). This approach was sensitive to the initial guess value and might return different joint estimated L and K at convergence. Each set of determined L and K were then used to calculate M following:

$$M = 4.118K^{0.73} \times L_\infty^{-0.33} \tag{1}$$

which was widely recommended as the most reliable estimator for M (Then et al., 2015). 200 sets of M estimates were generated for the period from 2011 to 2018.

These M estimates were then investigated for their relationships with the green tide bloom intensity of the same year. Due to the lack of a standardized bloom intensity index, we chose the distribution area of the green tide as the

FIGURE 2 | (A) Historical green tide intensity measured with distribution areas, where the intensities of the 12 historical documents are categorized into high (red), medium (yellow), and low (green) levels. **(B)** The linear relationship fitted between the log-transformed natural mortality and the green tide bloom intensity. **(C)** The values of natural mortality multiplier under the historical bloom intensity (indicated with the red dots).

intensity indicator. The bloom intensity would shape M via a multiplier to the baseline natural mortality rates (M_0) with the function (Harford et al., 2018):

$$BI_y = \log(\theta_y)/c \qquad (2)$$

where BI_y is bloom intensity in year y, θ is the multiplier, and c is a scaling constant. The M affected by blooms would be:

$$M_y = M_0 \cdot e^{c \cdot BI_y} \qquad (3)$$

where M_y is the shaped natural mortality rate, and M_0 is the baseline natural mortality rate set constantly at 0.2. Here we did not consider the age effect in natural mortality.

The parameterizations for Equations (2) and (3) were determined using the estimated M and the corresponding green tide bloom intensities in the historical years. Log-transformation was performed to Equation (3) to convert it into a linear model with ln (M_y) and BI_y being the responsive and explanatory variables, respectively. We then conducted a linear regression analysis as demonstrated in **Figure 2B**. The slope parameter was significantly different from zero ($P < 0.05$), indicating that the log-transformed natural mortality rate was positively related to the green tide intensity for each year. The established linear relationship was used in the following part of the study to deduce a consequent multiplier for M when different green tide bloom intensities were simulated (**Figure 2C**).

Simulation Framework

The employed simulation platform was essentially a closed-loop projection framework simplified from a fisheries population dynamic model (Sun et al., 2021a). The framework modeled the key ecological processes for the population including migration, spawning, mortality, and growth (**Figure 3**). The simulated fishery and stock were parameterized according to the small yellow croaker in the region, which was one of the four China's major domestic commercial fisheries (**Table 1**). The projection framework forwarded on a monthly time step and accounted for the management measures that were realistically applied in the region, including the 4-month summer moratorium (from the beginning of May to the end of August), the local no-fishing zone, and the mesh size limits regulated as the national standard (**Table 2**).

The natural mortality process was specifically enriched to accommodate the impact of green tides. Historical records indicated that the green tide occurred in a fairly consistent temporal pattern (Zhang Y. et al., 2019): it emerged at the beginning of May in a small scale, followed by a rapid escalation and maintained at peak level until the end of July. Therefore, we assumed full bloom intensity for June and July, and half intensity for May. The increase in M would occur at an annual level calculated with Equation (3), which was then allocated into May, June, and July proportionally according to the bloom intensity. Consequently, a bump in M would be formed within each year as a result of green tides (**Figure 3**). The height of the bump would be dictated by the bloom intensity. Note that we did not consider other factors influencing M so that the baseline M scenario free of green tide was a flat line.

Simulation Scenario

Projections were performed under a suite of scenarios featuring different green tide bloom intensities. The baseline scenario without green tide was set as a reference. We grouped the 12-year historical green tide bloom into high, medium, and low intensity levels and used them to set three corresponding simulation scenarios (**Figure 2**). The simulated stock was projected for 20 years for each of these scenarios. The projections were designed to be stochastic using the Monte Carlo approach (Arunraj et al.,
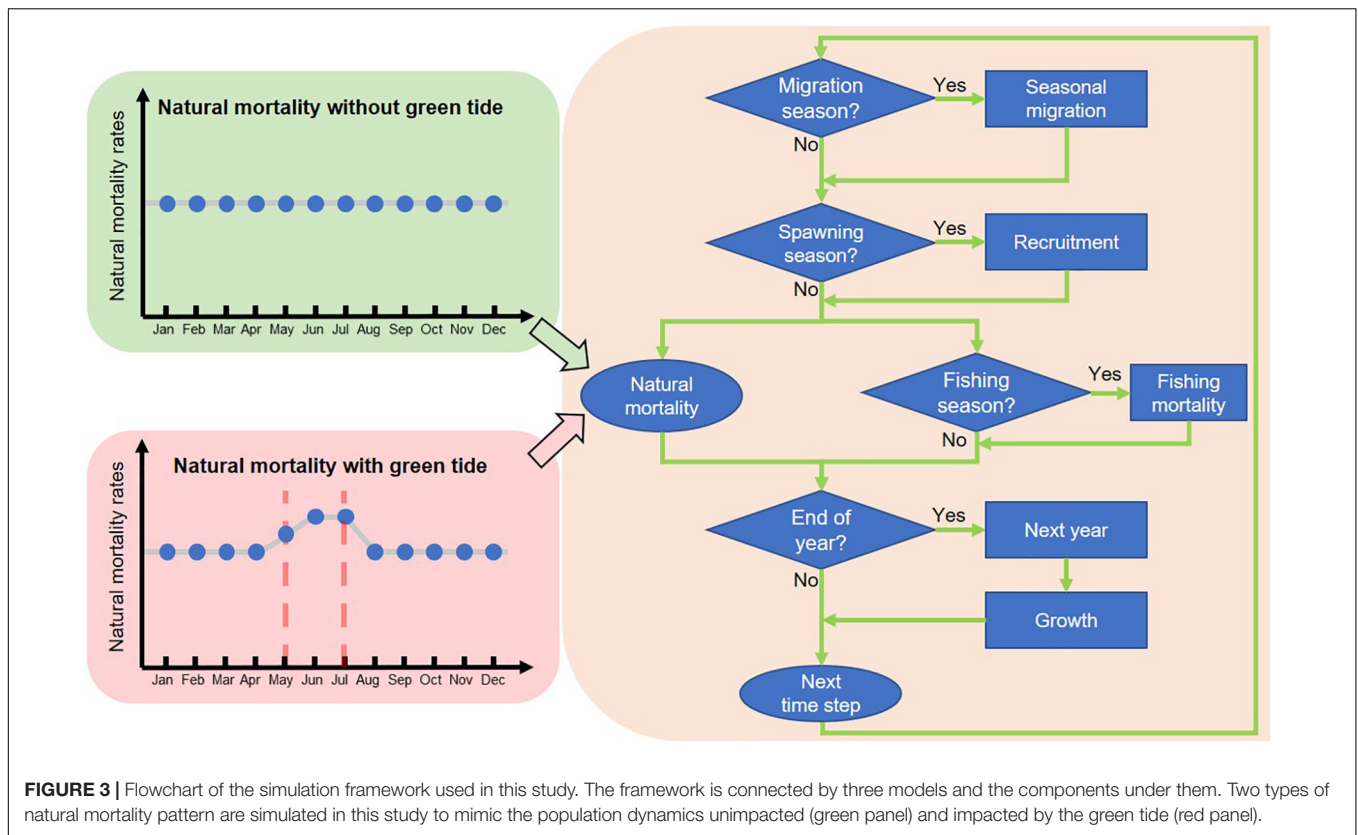
FIGURE 3 | Flowchart of the simulation framework used in this study. The framework is connected by three models and the components under them. Two types of natural mortality pattern are simulated in this study to mimic the population dynamics unimpacted (green panel) and impacted by the green tide (red panel).

2013), where the bloom intensity in each simulated year would be sampled from the distributions containing the corresponding historical intensities. The projections were iterated for 1,000 times. The intermediated time length (20 year) was deemed as an optimal temporal scale, because short-term projections would be too short to demonstrate the influence of green tides, while long-term projections might be less robust when neglecting dynamics from other drivers that could affect natural mortality, such as climate change. The fishing intensity was set constantly at a level that could lead to the (F_{MSY}). The values of F_{MSY} and MSY were determined from the baseline scenario (**Figure 4**) and applied to all scenarios, although the complications in M might render these estimations biased, which were revealed by the simulations.

Performance Metrics

The influence of green tides on the simulated fishery was evaluated with a set of metrics. We used the total stock biomass as the ecological indicator because it represented the status of fish population. Catch yielded by the fishery was also examined. The four scenarios were compared for their performance in final stock biomass and total catch over the simulation period. Considering that the onset of green tide would induce fish kills undesirable to management, it would be necessary to revisit the determination of optimal exploitation level under such circumstances. Therefore, we further investigated how fisheries management should adapt to the existence of green tides by recalculating the optimal fishing level F_{MSY} under different bloom intensities. This was achieved by plotting the catch at
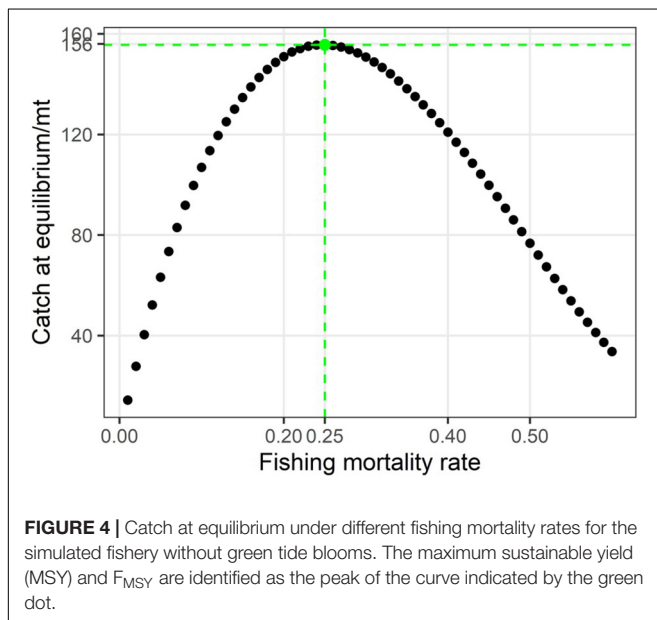
TABLE 1 | Population dynamics simulated with the projection model.

Process	Details
Migration	$N_{ts+1,i,a} = N_{ts,i,a} \times migration.factor$
	where N = abundance, ts = time step, i = patch, a = age,
	$migration.factor$ = 46.49% (November) and 161.33% (May)
Movement	$T_{ts,\,i}^{b} = \dfrac{T_{max}}{1 + Ae^{-\frac{\ln(A)}{B_i^*} \times S_{ts,i}}}$
	$T_{ts,i} = T_{ts,i}^{b} \times \dfrac{\frac{S_{ts,i}}{P_i}}{\sum \frac{S_{ts,i}}{P_i}} \times 2$
	where $T_{ts,\,i}^{b}$ is the basic movement rate for patch i in time step ts, $T_{ts,i}$ is the final movement rate, T_{max} is the maximum movement rate (1), A = 9, B_i^* indicates the carrying capacity of patch i measured with biomass (1460.75 and 65.62 mt), and $S_{ts,i}$ is SSB, P_i indicates the size of patch i (95.66 and 4.34% of the region)
Spawning	$R = \dfrac{\alpha \times S}{1 + \beta \times S}$
	where R = recruited age 1 abundance, S = spawning biomass, α = 0.1427, β = 2.56 * 10^{-9}
Mortality	$Z_{ts,i,a} = M_{ts,i,a} + F_{ts,i,a}$
	$N_{ts+1,i,a} = N_{ts,i,a} \times e^{Z_{ts,i,a}}$
	where Z = total mortality rate, M = natural mortality rate
Growth	$W_a = W_\infty \times (1 - e^{-k \times (a - t_0)})^3$
	where W = weight, W_∞ = asymptotic average weight, k = Brody growth rate, t_0 = theoretical age at zero weight

equilibrium under a wide gradient of fishing mortality rates and identifying the fishing mortality rates that corresponded to the peak value of the curve (**Figure 3**). The B_{MSY} and MSY derived from the recalculated optimal exploitation levels were compared

TABLE 2 | Management measures simulated for the fishery.

Measure	Details
Summer moratorium	Effective from the beginning of May to the end of August. During this period, fishing mortality rates are considered as 0 for the simulated fishery.
Local no-fishing zone	Effective year-round. Modeled with a two-patch spatial structure. The fishing mortality rates in the closed patch are 0. The size of the closed patch accounts for 4.34% of the study region (Li et al., 2019).
Mesh size limits	Effective year-round. The selectivity curve is shaped by this regulation. As a result of this, selectivity for age 1 is 0.45, while other age groups are fully selected (Sun et al., 2018a).

FIGURE 4 | Catch at equilibrium under different fishing mortality rates for the simulated fishery without green tide blooms. The maximum sustainable yield (MSY) and F_{MSY} are identified as the peak of the curve indicated by the green dot.

among the four scenarios. The final age-structures were also compared to demonstrate any potential age-dependent patterns. The projections to recalculate F_{MSY} were also iterated for 1000 times to account for the associated uncertainty in intensities of green tide blooms.

RESULTS

Biomass and Total Catch Under Various Green Tide Bloom Intensities

The simulated biomass and catch were demonstrated with their trajectories over the simulation period and final distributions for four simulation scenarios (**Figure 5**). In general, the occurrence of green tide strongly affected the stock biomass and total catch. The biomass trajectories fell consistently below the baseline scenario throughout the simulation (**Figure 5A**). The final biomass was reduced for the baseline scenario by approximately 100 mt (10%), 150 mt (15%), and 300 mt (>20%) when the intensities of green tide bloom were low, medium, and high, respectively (**Figure 5C**). The variations in biomass due to stochastic sampling were negligible, likely because the historical bloom levels were relatively similar within each intensity group. The trends and final distribution showed a pattern highly
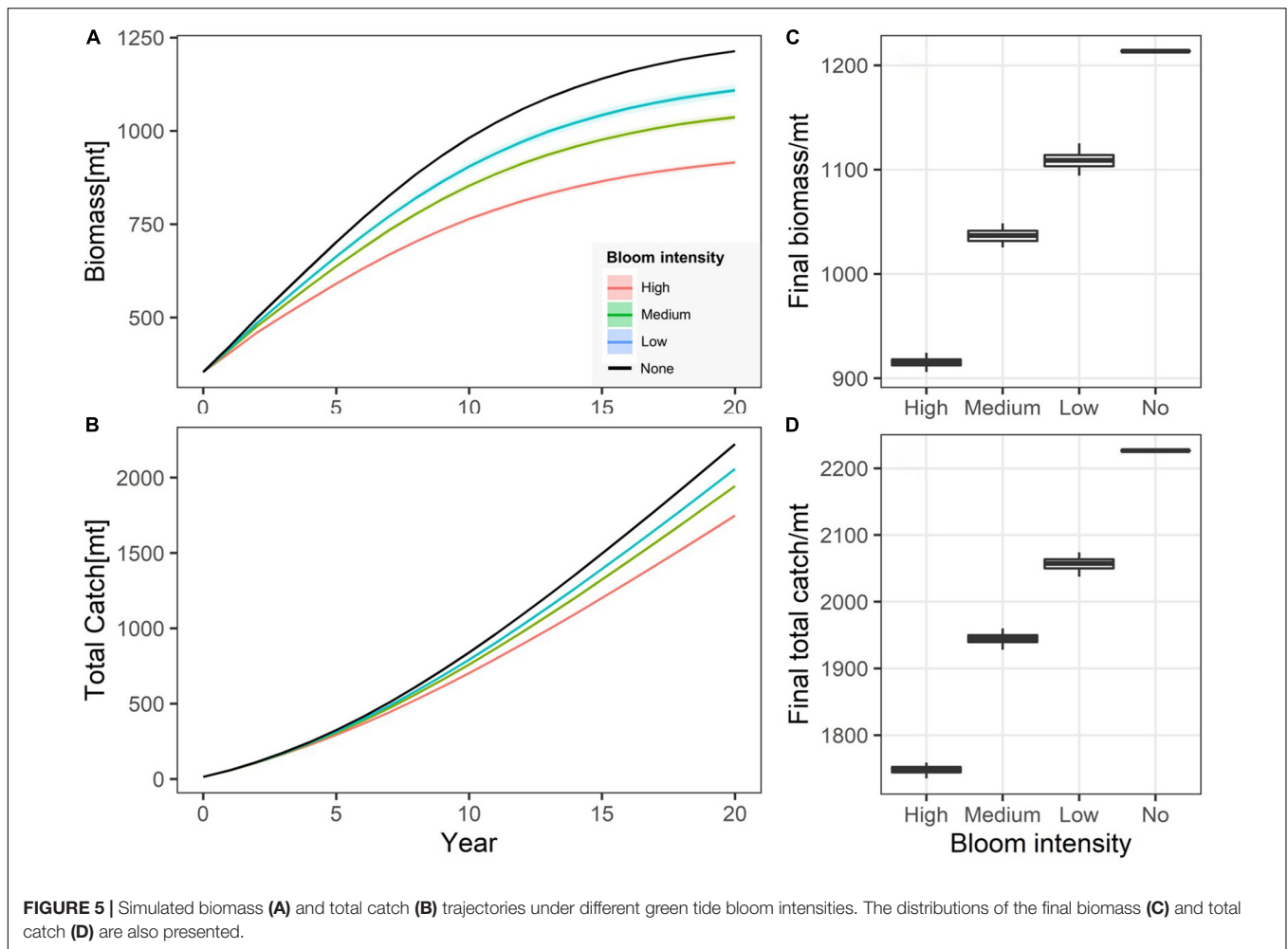
similar to that for biomass (**Figures 5B,D**), except that the disparity in the final total catch among different bloom intensities were much larger.

Maximum Sustainable Yield Reference Points Under Various Green Tide Bloom Intensities

The catch at equilibrium was plotted against the gradient of fishing mortality rates for four simulation scenarios to determine the scenario specific F_{MSY} and MSY (**Figure 6**). MSY was determined as the peak value of the curve, while F_{MSY} was the fishing mortality rate corresponding to the peak. Compared to the original value defined from the baseline scenario free of green tide at 0.25, the adjusted values of F_{MSY} in the context of green tide were reduced to 0.24, 0.24, and 0.23 when the intensities of green tide bloom were low, medium, and high, respectively. However, the values of MSY were greatly reduced for approximately 20, 30, and 40 mt for the low, medium, and high scenarios, respectively. The biomass at equilibrium (B_{MSY}) was also strongly reduced for these scenarios (**Figure 7**). Specifically, the median B_{MSY} estimated under the low, medium, and high green tide bloom intensities were 1,195, 1,122, and 1,034 mt, respectively, compared to the baseline scenario at 1,263 mt. The variations in B_{MSY} were also negligible. The age structure at equilibrium was compared for the four scenarios (**Figure 8**). The abundance-at-age was reduced as the intensity of green tide increased from low to high. However, the age structure was not truncated by the occurrence of green tide at any intensity, indicating that the consequent surge in natural mortality did not accumulate over age when age-specific mortality was not accounted for.

DISCUSSION

Overall, green tides proved to affect fisheries in the Southern Yellow Sea in two ways: (1) they cause losses to fishery by reducing population biomass and catch, and (2) they force the targets of sustainable fisheries to be redefined to mitigate their negative effects. Projection results demonstrated that losses in stock biomass and total catch were obvious even at low bloom intensity when fishing at the pre-defined F_{MSY}, which was regarded as the optimal exploitation level without green tides. This finding underscores the risk of ignoring green tides in fisheries management and the necessity to redefine sustainable targets under such circumstances. This conclusion aligns with the simulation results from Harford et al. (2018), which report

FIGURE 5 | Simulated biomass **(A)** and total catch **(B)** trajectories under different green tide bloom intensities. The distributions of the final biomass **(C)** and total catch **(D)** are also presented.

an increased risk of overfishing and the stock being overfished when blooms are not considered during setting catch limits. This study also revisited the threshold of sustainable management approaches by reevaluating MSY, which was the most important reference point in fisheries.

Effects of Green Tides Bloom to Maximum Sustainable Yield

Variations in the F_{MSY} and MSY were observed when assessing the management effects at equilibrium under different fishing mortality rates. The reductions in F_{MSY} were minor, while reductions in B_{MSY} and MSY were much larger, indicating that the damages caused by green tides could only be partially compensated by reducing exploitation rates. Harford et al. (2018) tested precautionary and reactive modifications to the original strategies as two management alternatives for the Gulf of Mexico red grouper assuming that dynamics of blooms could be unpredictable and that F_{MSY} could be difficult to estimate. These two approaches showed trade-offs between catch and biomass, which are identical to our observation from the adjusted F_{MSY} curve (**Figure 6**). Age structures were not truncated by green tides, mainly because we did not incorporate age-specific

mortality effects in our simulation. The age-unspecific model design is adequate, given that there is currently a lack of supportive materials addressing the age-dependent vulnerability of fish to green tides or similar HABs.

Fisheries Modeling in the Context of Green Tides Bloom

Modeling the occurrence of green tide as a periodically recurring event causing surge in natural mortality is a feasible approach to accommodate green tide in fisheries stock assessment and management. Linking fish kills to natural mortality is straightforward and can avoid introducing additional processes as well as uncertainty that may be hard to quantify (Burkholder, 1998; Glaser et al., 2014).

There are two factors that need to be considered when contemplating the natural mortality event related to HABs. First, the natural mortality event may have different characteristics under different temporal resolutions. Fisheries assessment models pervasively assume constant natural mortality rates due to the difficulty in estimating their values (Johnson et al., 2015). In this case, the occurrence of green tides would result in episodic natural mortality fluctuations that are unable to be specified
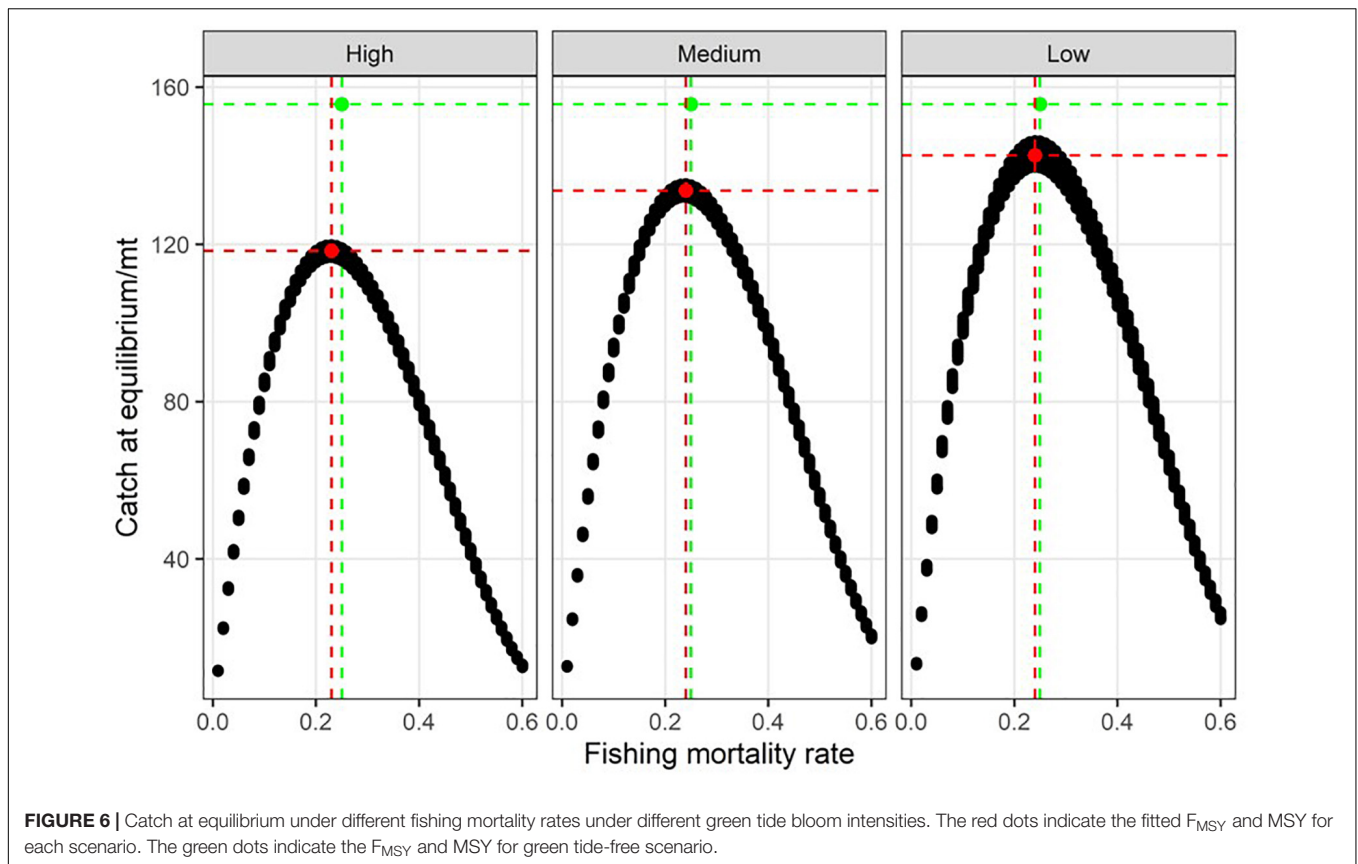
FIGURE 6 | Catch at equilibrium under different fishing mortality rates under different green tide bloom intensities. The red dots indicate the fitted F_{MSY} and MSY for each scenario. The green dots indicate the F_{MSY} and MSY for green tide-free scenario.
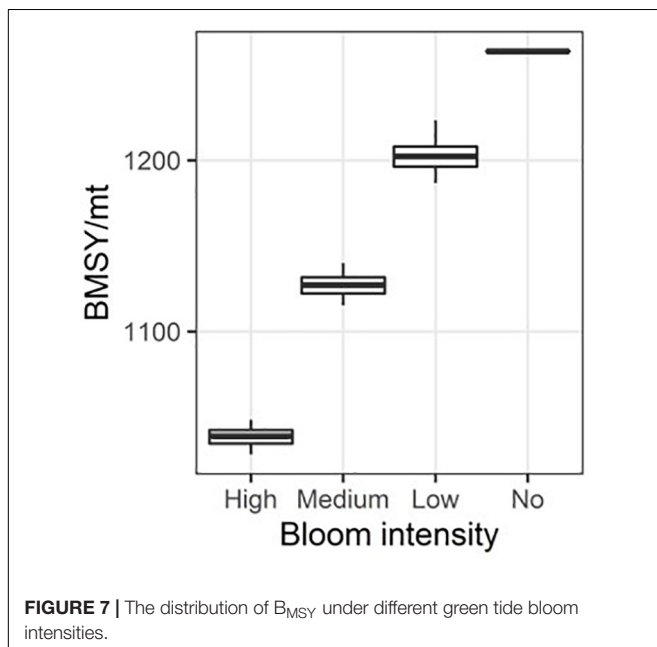

FIGURE 7 | The distribution of B_{MSY} under different green tide bloom intensities.

for their magnitudes with the annual level stock assessment. Nevertheless, many HABs have relatively consistent seasonal patterns, such as green tides in the Southern Yellow Sea and the summer-long HAB in the Lake Erie, which may result in

seasonal surge in natural mortality rates to fish populations (Wolf et al., 2017; Zhang Y. et al., 2019). It is not only meaningful but also realistic to reconcile the interannual and interseason characteristics. In this study, we achieved this task by linking annual natural mortality rates to the intensity of green tides bloom and specifying the seasonality of surge in natural mortality. Specifically, we estimated natural mortality rates for separated years based on growth parameters (Then et al., 2015) and performed projections with month time-steps to reflect the bloom seasonality. This approach is applicable to other fisheries with similar issues.

The second factor that needs to be addressed is the quantification of HAB intensity. Standardized intensity indicators are necessary to develop comprehensive fisheries management strategies as suggested by previous practices (Walter et al., 2013; Southeast Data, Assessment, and Review [SEDAR], 2015). Due to the limited data with fisheries and green tides, the size of the distribution area of *U. prolifera* is the only reliable and coherent indicator among years (Zhang Y. et al., 2019). Although the positive relationship between annual natural mortality rates and the size of distribution area is significant ($P < 0.05$), the predicting ability of such relationship still needs to be justified with more years of documentations. Modeling the spatial overlap of fish distribution and green tide coverages and tracing multispecies interactions may also be promising approaches to link HABs effects to single-species fisheries management (Walter et al., 2013; Sagarese et al., 2014; Grüss
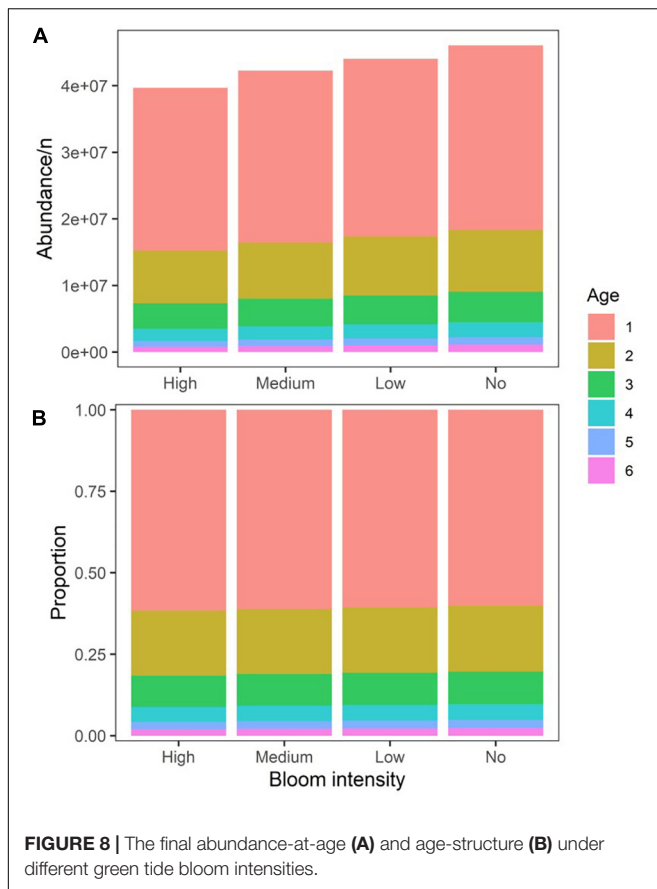
FIGURE 8 | The final abundance-at-age **(A)** and age-structure **(B)** under different green tide bloom intensities.

et al., 2016). However, these approaches are data intensive and require the underlying models to be developed. There need to be achieved by developing more comprehensive survey station designs to fill the gaps in spatial coverages of green tides and fisheries-independent survey. Despite this, it is still critical to implement the "best available science" to develop more proactive management actions to ensure sustainable fisheries in the face of green tides (Burkholder, 1998; Sullivan et al., 2006; Harford et al., 2018).

Fisheries Management in the Context of Green Tides Bloom

Current management measures imposed on the fisheries in the Southern Yellow Sea are considered in the simulation, including summer moratorium, spatial closure, and mesh size limits. These measures are not originally implemented to counter green tides, and do not even constitute a robust management system against other sources of uncertainties (Sun et al., 2021b). The summer moratorium in China is the largest and most comprehensive temporal fisheries closure in the world, lasting 4 months from May 1st to August 31st in the Yellow Sea. This closure period perfectly overlaps with the genesis, development, and flourishing or the green tides (Zhang Y. et al., 2019), whose damage to the fish populations as well as the marine ecosystem might have been partially offset. If the fishing efforts in summer are not constrained by the summer closure, fish populations

in the Yellow Sea could suffer higher mortality rates due to the combinational effects from intensive fishing and green tide blooms. It is also possible that fishing vessels would not be able to operate in the region covered by algal mats, resulting in reduction in catches. Either way, the temporal overlap of fishing and green tides would result in substantial ecological and socio-economic loss. Nevertheless, the summer closure in China has rarely been systematically described or discussed for its conservation contributions to fisheries (Xing et al., 2020).

Although the current management measures may alleviate the adverse effects of green tides on fisheries to a certain extent, specific management guidance still needs to be developed to ensure sustainable fisheries management under the recurring surge in natural mortality. Narratives provided by Harford et al. (2018) depict an applicable roadmap to modify the setting of catch limits for fisheries with extensive stock assessment and database. To achieve similar tasks in the Yellow Sea, three issues must be resolved. First, the current data condition of fisheries can only support management modifications based on data-limited methods and management procedures (Sun et al., 2018a), which requires further modifications in methodologies to account for surges in natural mortality at a finer temporal scale. Second, modeling the linkage between green tides and fisheries also requires more analysis on remote sensing and ecology data to establish standardized indicators that can be used in fisheries modeling and assessment (Anderson et al., 2001; Walter et al., 2013). Besides inducing increasing mortality to fish populations, green tides can also provide food source and spawning places for many marine organisms, which complicates the interaction between green tides and fish population dynamics (Liu et al., 2020). Last but not the least, future dynamics of green tide blooms in the Southern Yellow Sea may be unpredictable and hard to be explicitly considered in fisheries management decision making. Specifically, environmental factors such as water temperature, nitrogen concentration (eutrophication), and thermal conditions prove influential to the occurrence of green tides in a complex manner (Cui et al., 2015; Gao et al., 2017). However, it has been confirmed that these factors are subject to changes due to climate changes and human activity in the coastal China region (Ma et al., 2019). Future studies dedicated to achieving sustainable fisheries management against green tides and HABs must address these issues by incorporating related factors into not only stock assessment but also monitoring design.

DATA AVAILABILITY STATEMENT

The original contributions presented in the study are included in the article/supplementary material, further inquiries can be directed to the corresponding author.

AUTHOR CONTRIBUTIONS

MS: study conception and design and manuscript draft preparation. MS, YL, and YR: data collection. MS, YL, and YC: analysis and interpretation of results and editing and reviewing

REFERENCES

Anderson, D. M., Andersen, P., Bricelj, V. M., Cullen, J. J., and Rensel, J. E. (2001). *Monitoring and Management Strategies for Harmful Algal Blooms in Coastal Waters*. Paris: Intergovernmental Oceanographic Commission.

Arunraj, N., Mandal, S., and Maiti, J. (2013). Modeling uncertainty in risk assessment: an integrated approach with fuzzy set theory and Monte Carlo simulation. *Accid. Anal. Prev.* 55, 242–255. doi: 10.1016/j.aap.2013.03.007

Backer, L. C. (2009). Impacts of Florida red tides on coastal communities. *Harmful Algae* 8, 618–622. doi: 10.1016/j.hal.2008.11.008

Beverton, R. J. H., and Holt, S. J. (1957). *On the Dynamics of Exploited Fish Populations*. Great Britain: Ministry of Agriculture, Fisheries and Food.

Brodziak, J., Ianelli, J. N., Lorenzen, K., and Methot, R. D. (2011). *Estimating Natural Mortality in Stock Assessment Applications*. Washington: NOAA.

Burkholder, J. A. M. (1998). Implications of harmful microalgae and heterotrophic dinoflagellates in management of sustainable marine fisheries. *Ecol. Appl.* 8, S37–S62. doi: 10.2307/2641362

Cruz-Rivera, E., Flores-Diaz, M., and Hawkins, A. (2015). A fish kill coincident with dense Sargassum accumulation in a tropical bay. *Bull. Mar. Sci.* 91, 455–456. doi: 10.5343/bms.2015.1048

Cui, J., Zhang, J., Huo, Y., Zhou, L., Wu, Q., Chen, L., et al. (2015). Adaptability of free-floating green tide algae in the Yellow Sea to variable temperature and light intensity. *Mar. Pollut. Bull.* 101, 660–666. doi: 10.1016/j.marpolbul.2015.10.033

Gao, G., Clare, A. S., Rose, C., and Caldwell, G. S. (2017). Eutrophication and warming-driven green tides (*Ulva rigida*) are predicted to increase under future climate change scenarios. *Mar. Pollut. Bull.* 114, 439–447. doi: 10.1016/j.marpolbul.2016.10.003

Glaser, S. M., Fogarty, M. J., Liu, H., Altman, I., Hsieh, C. H., Kaufman, L., et al. (2014). Complex dynamics may limit prediction in marine fisheries. *Fish Fish.* 15, 616–633. doi: 10.1111/faf.12037

Glibert, P. M., Icarus Allen, J., Artioli, Y., Beusen, A., Bouwman, L., Harle, J., et al. (2014). Vulnerability of coastal ecosystems to changes in harmful algal bloom distribution in response to climate change: projections based on model analysis. *Glob. Chang. Biol.* 20, 3845–3858. doi: 10.1111/gcb.12662

Grüss, A., Harford, W. J., Schirripa, M. J., Velez, L., Sagarese, S. R., Shin, Y.-J., et al. (2016). Management strategy evaluation using the individual-based, multispecies modeling approach OSMOSE. *Ecol. Modell.* 340, 86–105. doi: 10.1016/j.ecolmodel.2016.09.011

Harford, W. J., Grüss, A., Schirripa, M. J., Sagarese, S. R., Bryan, M., and Karnauskas, M. (2018). Handle with care: establishing catch limits for fish stocks experiencing episodic natural mortality events. *Fisheries* 43, 463–471. doi: 10.1002/fsh.10131

Imai, I., and Yamaguchi, M. (2012). Life cycle, physiology, ecology and red tide occurrences of the fish-killing *raphidophyte Chattonella*. *Harmful Algae* 14, 46–70. doi: 10.1016/j.hal.2011.10.014

Imai, I., Yamaguchi, M., and Hori, Y. (2006). Eutrophication and occurrences of harmful algal blooms in the Seto Inland Sea, Japan. *Plankt. Benthos Res.* 1, 71–84. doi: 10.3800/pbr.1.71

Jin, D., and Hoagland, P. (2008). The value of harmful algal bloom predictions to the nearshore commercial shellfish fishery in the Gulf of Maine. *Harmful Algae* 7, 772–781. doi: 10.1016/j.hal.2008.03.002

Johnson, K. F., Monnahan, C. C., McGilliard, C. R., Vert-pre, K. A., Anderson, S. C., Cunningham, C. J., et al. (2015). Time-varying natural mortality in fisheries stock assessment models: identifying a default approach. *ICES J. Mar. Sci.* 72, 137–150. doi: 10.1093/icesjms/fsu055

Lewitus, A. J., Horner, R. A., Caron, D. A., Garcia-Mendoza, E., Hickey, B. M., Hunter, M., et al. (2012). Harmful algal blooms along the North American West Coast region: history, trends, causes, and impacts. *Harmful Algae* 19, 133–159. doi: 10.1016/j.hal.2012.06.009

Li, Y., Zhang, C., Xue, Y., Xu, B., Sun, M., Ren, Y., et al. (2019). Developing a marine protected area network with multiple objectives in China. *Aquat. Conserv. Mar. Freshw. Ecosyst.* 29, 952–963. doi: 10.1002/aqc.3076

Liu, D., Keesing, J. K., Dong, Z., Zhen, Y., Di, B., Shi, Y., et al. (2010). Recurrence of the world's largest green-tide in 2009 in Yellow Sea, China: *Porphyra yezoensis* aquaculture rafts confirmed as nursery for macroalgal blooms. *Mar. Pollut. Bull.* 60, 1423–1432. doi: 10.1016/j.marpolbul.2010.05.015

Liu, D., Keesing, J. K., He, P., Wang, Z., Shi, Y., and Wang, Y. (2013). The world's largest macroalgal bloom in the Yellow Sea, China: formation and implications. *Estuar. Coast. Shelf Sci.* 129, 2–10. doi: 10.1016/j.ecss.2013.05.021

Liu, J., Tong, Y., Xia, J., Sun, Y., Zhao, X., Sun, J., et al. (2022). *Ulva* macroalgae within local aquaculture ponds along the estuary of Dagu River, Jiaozhou Bay, Qingdao. *Mar. Pollut. Bull.* 174:113243. doi: 10.1016/j.marpolbul.2021.113243

Liu, J., Xia, J., Zhuang, M., He, P., Sun, Y., Tong, Y., et al. (2021a). Golden seaweed tides accumulated in *Pyropia* aquaculture areas are becoming a normal phenomenon in the Yellow Sea of China. *Sci. Total Environ.* 774:145726. doi: 10.1016/j.scitotenv.2021.145726

Liu, J., Xia, J., Zhuang, M., Zhang, J., Yu, K., Zhao, S., et al. (2021b). Controlling the source of green tides in the Yellow Sea: NaClO treatment of Ulva attached on *Pyropia* aquaculture rafts. *Aquaculture* 535:736378. doi: 10.1016/j.aquaculture.2021.736378

Liu, J., Li, C., Xia, J., Sun, Y., Tong, Y., Zhang, J., et al. (2021c). Epizoic Ulva attached to intertidal animals in the Subei intertidal zone are not the additional source of the famed Yellow Sea green tides. *J. Sea Res.* 174:102065. doi: 10.1016/j.seares.2021.102065

Liu, J., Zhuang, M., Zhao, L., Liu, Y., Wen, Q., Fu, M., et al. (2020). Taxonomy and genetic diversity of amphipods living on *Ulva lactuca* L. in Gouqi coast of China. *Pac. Sci.* 74, 137–146. doi: 10.2984/74.2.3

Ma, S., Liu, Y., Li, J., Fu, C., Ye, Z., Sun, P., et al. (2019). Climate-induced long-term variations in ecosystem structure and atmosphere-ocean-ecosystem processes in the Yellow Sea and East China Sea. *Prog. Oceanogr.* 175, 183–197. doi: 10.1016/j.pocean.2019.04.008

MARA (2018). *China Fishery Statistical Yearbook 2018*. Beijing: China Statistics press.

McCabe, R. M., Hickey, B. M., Kudela, R. M., Lefebvre, K. A., Adams, N. G., Bill, B. D., et al. (2016). An unprecedented coastwide toxic algal bloom linked to anomalous ocean conditions. *Geophys. Res. Lett.* 43, 10366–10376. doi: 10.1002/2016GL070023

Sagarese, S. R., Tetzlaff, J. C., Bryan, M. D., Walter, J. F., and Schirripa, M. J. (2014). *Linking an Environmental Index to Natural Mortality Within the Stock Synthesis Integrated Assessment Model Framework: A Case Study for Gulf of Mexico Gag Grouper (Mycteroperca microlepis) and Red Tide*. North Charleston: SEDAR.

Southeast Data, Assessment, and Review [SEDAR] (2015). *Stock Assessment Report: Gulf of Mexico Red Grouper*. North Charleston: SEDAR.

Sullivan, P. J., Acheson, J. M., Angermeier, P. L., Faast, T., Flemma, J., Jones, C. M., et al. (2006). Defining and implementing best available science for fisheries and environmental science, policy, and management. *Fisheries* 31, 460–465. doi: 10.1100/tsw.2002.191

Sun, M., Li, Y., Ren, Y., and Chen, Y. (2021a). Developing an intermediate-complexity projection model for China's fisheries: a case study of small yellow croaker (*Larimichthys polyactis*) in the Haizhou Bay, China. *Acta Oceanol. Sin.* 40, 108–118. doi: 10.1007/s13131-021-1793-3

Sun, M., Li, Y., Ren, Y., and Chen, Y. (2021b). Rebuilding depleted fisheries towards BMSY under uncertainty: harvest control rules outperform combined management measures. *ICES J. Mar. Sci.* 78, 2218–2232. doi: 10.1093/icesjms/fsaa078

Sun, M., Zhang, C., Chen, Y., Xu, B., Xue, Y., and Ren, Y. (2018a). Assessing the sensitivity of data-limited methods (DLMs) to the estimation of life-history parameters from length–frequency data. *Can. J. Fish. Aquat. Sci.* 75, 1563–1572. doi: 10.1139/cjfas-2017-0325

Sun, M., Zhang, C., Li, Y., Xu, B., Xue, Y., and Ren, Y. (2018b). Management strategy evaluation of fishery stocks in Haizhou Bay based on Data-Limited Methods. *J. Fish. China* 42, 1661–1669. doi: 10.11964/jfc.20170910964

Sun, S., Wang, F., Li, C., Qin, S., Zhou, M., Ding, L., et al. (2008). Emerging challenges: massive green algae blooms in the Yellow Sea. *Nat. Prec.* doi: 10.1038/npre.2008.2266.1

Taylor, M. H., and Mildenberger, T. K. (2017). Extending electronic length frequency analysis in R. *Fish. Manag. Ecol.* 24, 330–338. doi: 10.1111/fme.12232

Then, A. Y., Hoenig, J. M., Hall, N. G., and Hewitt, D. A. (2015). Evaluating the predictive performance of empirical estimators of natural mortality rate using information on over 200 fish species. *ICES J. Mar. Sci.* 72, 82–92. doi: 10.1093/icesjms/fsu136

Walter, J. F., Christman, M. C., Landsberg, J. H., Linton, B., Steidinger, K., Stumpf, R., et al. (2013). *Satellite Derived Indices of Red Tide Severity for Input for Gulf of Mexico Gag Grouper Stock Assessment.* North Charleston: SEDAR.

Wang, Y., Wang, Y., Liu, S., Liang, C., Zhang, H., and Xian, W. (2020). Stock assessment using LBB method for eight fish species from the Bohai and Yellow Seas. *Front. Mar. Sci.* 7:164. doi: 10.3389/fmars.2020.00164

Ward, C. H., and Tunnell, J. W. (2017). "Habitats and biota of the Gulf of Mexico: an overview," in *Habitats and Biota of the Gulf of Mexico: Before the Deepwater Horizon Oil Spill*, ed. C. Ward (New York: Springer), 1–54. doi: 10.1007/978-1-4939-3447-8_1

Wolf, D., Georgic, W., and Klaiber, H. A. (2017). Reeling in the damages: harmful algal blooms' impact on Lake Erie's recreational fishing industry. *J. Environ. Manage.* 199, 148–157. doi: 10.1016/j.jenvman.2017.05.031

Xing, L., Chen, Y., Zhang, C., Li, B., Shin, Y. J., and Ren, Y. (2020). Evaluating impacts of pulse fishing on the effectiveness of seasonal closure. *Acta Oceanol. Sin.* 39, 89–99. doi: 10.1007/s13131-020-1536-x

Xing, Q., Tosi, L., Braga, F., Gao, X., and Gao, M. (2015). Interpreting the progressive eutrophication behind the world's largest macroalgal blooms with water quality and ocean color data. *Nat. Hazards* 78, 7–21. doi: 10.1007/s11069-015-1694-x

Xu, B., Zhang, C., Xue, Y., Ren, Y., and Chen, Y. (2015). Optimization of sampling effort for a fishery-independent survey with multiple goals. *Environ. Monit. Assess.* 187:252. doi: 10.1007/s10661-015-4483-9

Ye, N. H., Zhang, X. W., Mao, Y. Z., Liang, C. W., Xu, D., Zou, J., et al. (2011). 'Green tides' are overwhelming the coastline of our blue planet: taking the world's largest example. *Ecol. Res.* 26, 477–485. doi: 10.1007/s11284-011-0821-8

Zhang, J., Liu, C., Yang, L., Gao, S., Ji, X., Huo, Y., et al. (2015). The source of the *Ulva* blooms in the East China Sea by the combination of morphological, molecular and numerical analysis. *Estuar. Coast. Shelf Sci.* 164, 418–424. doi: 10.1016/j.ecss.2015.08.007

Zhang, J., Shi, J., Gao, S., Huo, Y., Cui, J., Shen, H., et al. (2019). Annual patterns of macroalgal blooms in the Yellow Sea during 2007-2017. *PLoS One* 14:e0210460. doi: 10.1371/journal.pone.0210460

Zhang, Y., He, P., Li, H., Li, G., Liu, J., Jiao, F., et al. (2019). *Ulva* prolifera green-tide outbreaks and their environmental impact in the Yellow Sea, China. *Natl. Sci. Rev.* 6, 825–838. doi: 10.1093/nsr/nwz026

Zhou, M. J., Liu, D. Y., Anderson, D. M., and Valiela, I. (2015). Introduction to the Special Issue on green tides in the Yellow Sea. *Estuar. Coast. Shelf Sci.* 163, 3–8. doi: 10.1016/j.ecss.2015.06.023

Zhuang, M., Liu, J., Ding, X., He, J., Zhao, S., Wu, L., et al. (2021). *Sargassum* blooms in the East China Sea and Yellow Sea: formation and management. *Mar. Pollut. Bull.* 162:111845. doi: 10.1016/j.marpolbul.2020.111845